UWB GROUND-PENETRATING RADAR SYSTEM FOR LANDMINE DETECTION

J.B. RHEBERGEN, A.P.M. ZWAMBORN AND A.T.M. WILBERS

TNO Physics and Electronics Laboratory P.O. Box 96864 2509 JG THE HAGUE The Netherlands Tel: +31-70-374 0772 e-mail: Rhebergen@fel.tno.nl

ABSTRACT

At TNO-FEL, one of the research programs is to explore the use of ultra-wideband (UWB) electromagnetic fields in a bi-static ground-penetrating radar (GPR) system for the detection, location and identification of buried items of unexploded ordnance (e.g. land mines). In the present paper we describe the current status of the development of this system.

The UWB ground-penetrating radar system is designed to operate in the frequency band from 200 MHz to 3 GHz and uses impulse radiating antennas (IRAs) as transponders to radiate and receive very short electromagnetic pulses from a short distance above the soil. The radiation IRA is driven by a pulse generator with a double exponential voltage waveform with a pulse rise time of 90 ps, a pulse width (FWHM) of 3 ns and a peak positive amplitude of 9 kV. The receiving IRA is similar to the transmitting IRA and is connected to a receiving unit which comprises of an attenuator, time gate switch, trigger delay generator and a sampling oscilloscope A personal computer is used to control the equipment. Finally, we present some results recorded at our full-size experimenting and testing facility.

SYSTEM DESIGN

To design an UWB GPR system for detection, location and identification of land-mines the following points have to be successfully combined.

- generation of UWB EM field (i.e. source)
- radiation of UWB EM field (i.e. antenna)
- characterization of the soil and air/earth interface
- reception and synthesis of scattered fields
- signal processing techniques and identification of objects
- controlled experimental/test environment

An overview of the overall system concept is shown in figure 1. The target volume is illuminated by an ultra-wideband electromagnetic field, with an angle of incidence chosen to maximize energy transmission into the ground, whilst minimizing reflection from the ground/air

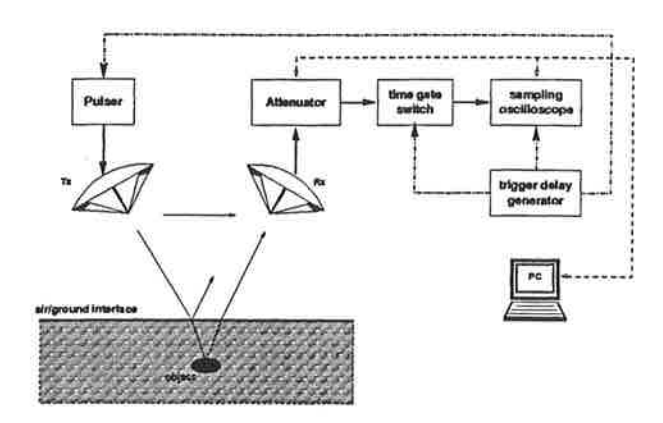


FIGURE 1 - Schematic block diagram of a generic UWB GPR system

interface. Presently, the main interest is in objects varying in size from about 5 cm up to ca. 75 cm. In air this corresponds to wavelengths of 1.5 m to 0.1 m. Consequently the frequency range of interest extends from 200 MHz up to 3 GHz.

The principal goal is to perform the needed analytical and design work to support the construction of an experimental/test facility, where targets can be buried in a sand medium and illuminated by an ultra-wideband electromagnetic field. The scattered fields have to be observed and diagnosed for the purpose of building an electronic database containing the responses of a large number of buried objects.

Generation of UWB EM fields

For our UWB GPR system it was decided to use a solid state pulse generator with a double exponential voltage waveform. Such a waveform can be modeled by,

$$V(t) = V_0\{\exp(-\beta t) - \exp(-\alpha t)\}u(t), \qquad (1)$$

with V_0 , α and β known constants, $\alpha >> \beta$ and u(t) the Heaviside step function. In our case the parameters are

$$V_0 = 9.635 \,\text{kV},$$
 (2)

$$\alpha = 2 \cdot 10^{10} \,\mathrm{s}^{-1} \,\mathrm{and} \,\beta = 2.5 \cdot 10^8 \,\mathrm{s}^{-1}.$$
 (3)

This gives rise to the following Fourier spectrum,

$$\tilde{V}(j\omega) = V_0 \left[\frac{1}{j\omega + \beta} - \frac{1}{j\omega + \alpha} \right].$$
 (4)

Since the magnitude of the far field is proportional to the derivative of the voltage waveform, a better

radiated spectrum (enhanced bandwidth) is obtained when compared to sinusoidal mono-cycles. The pulser is designed to drive a $50\,\Omega$ load, is fully protected against open and shortcircuit loads and has a pulse repetition frequency of 1 kHz. The pulse has a $10\,\%$ to $90\,\%$ rise time of about $100\,\mathrm{ps}$ and a full-width half-maximum (FWHM) time of 3 ns.

Radiation of UWB EM fields

Many commercially available wideband antennas have poor performance when it comes to radiating very short pulses. Part of the UWB GPR system design entailed the design of an IRA for ground penetrating radar applications. The upper frequency limit f_{upper} of such an antenna is determined by the pulse rise time t_{rise} while the lower frequency limit f_{lower} is determined by the dimensions of the reflecting dish. Pulse rise times of 25 ps and upper frequency limits of 20 GHz have been demonstrated in IRA designs. Experiments have shown that an antenna with a 4m reflecting dish and a 60 kV switch with a 85 ps rise time has a bandwidth extending from 35 MHz to 4 GHz with a field stength of 4 kV/m at 300 m. The frequency range of interest in our case is from about 200 MHz to 3 GHz. Hence the diameter of the reflecting dish was proposed to be in the order of 1 m.

Soil characterization

Electromagnetic waves are dampened considerably when traveling through a medium with a conductivity greater than zero. In our experimental set-up the angle of incidence and incident polarization are chosen such as to maximize the energy transfer from the transmitter into the ground. This is based on the technique of pulse matching into the ground developed in [10], for vertical polarization. If frequencies are much larger than the relaxation frequency of the ground $(f_{relax} = \sigma/\epsilon)$, there is an angle of incidence at which there is very little reflection of the incident wave from the air/ground interface. This is called the high-frequency Brewster angle. For $f >> f_{relax}$ it can be shown that reflection is minimal (theoretically zero) when,

$$\tan(\psi_B) = \sqrt{\epsilon_r}.\tag{5}$$

When $\sigma=0.01\,\mathrm{S/m}$ and $\epsilon_r=10$, then the relaxation frequency of the ground $f_{relax}=113\,\mathrm{MHz}$. Hence when the conductivity $\sigma\leq0.01\,\mathrm{S/m}$, which is quite typical, the radiated spectrum of the IRA will be transmitted into the ground with minimum reflection. The next table shows some examples of high-frequency Brewster angles at various values of permittivity.

ϵ_r	2	4	6	8	10
ψ_B	54.73°	63.42°	67.79°	70.53°	72.45°

Reception and synthesis of scattered fields

The receiving system consist of:

- receiving antenna, similar to transmitting antenna;
- processing unit (data acquisition).

The processing unit has to perform two tasks:

- recording and preprocessing the incoming signal, reducing noise, clutter and distortion caused by the signal path;
- perform some signal processing on the scattered field in order to be able to identify the buried objects.

Data acquisition and processing is done by a sampling (digitizing) oscilloscope able to perform measurements on signals with bandwidth of up to 20 GHz. The input signal cannot be measured reliably at just one instance, which is why a sampling oscilloscope employs a repetitive sampling architecture. This in turn requires the transmitted pulse to be repetitive as well. Arithmetic averaging of the repetitive input signal can significantly reduce the noise (and jitter) on the received scattered field signal. Gating allows isolation of the part of the signal due to the buried objects.

Signal processing and identification

Until 1980, almost all of the work in the field of ground-penetrating radar was directed towards the detection of buried objects. Only very few attempted the problem of target identification (or classification), which is a problem far more severe than the identification of aerospace targets by conventional radars where the target can literally be seen and the class of false targets is limited in scope. Underground there are varieties of undesired targets that complicate the task. Furthermore, the ground medium involved, is usually lossy, inhomogeneous and electrically weather-dependent. These problems, together with the presence of the air-ground interface, makes the task of subsurface target identification truly formidable.

It was suggested by some authors that the so-called singularity expansion method (SEM) is one of the few methods capable of performing identification of objects [2]. This method is based on the theoretical observation that all objects have natural resonant frequencies that depend on their size, shape and the material decomposition only and not on the orientation of the object or on the direction of the incoming field. When a target is hit by a short electromagnetic pulse, the target will "ring" and radiate a scattered field that contains as prominent constituents a set of damped sinusoids. These sinusoids represent the natural resonant frequencies. The bandwidth of the ultra-wideband system must be large enough to cover all the resonant frequencies of interest. The SEM will be exploited in the current problem of classification of the buried object for the calculation of the internal resonances of the buried object by processing the reflections or backscattering from the objects. Some initial analysis with synthetic data has already been performed [1].

DESIGN AND CONSTRUCTION OF AN IRA

The paraboloidal reflector antenna fed by a pyramidal horn has found wide-spread application in radar and communication engineering. The reflector antenna also has very useful characteristics when it is fed by two or four conductor transmission lines. A dispersion-less wideband antenna with a nearly flat radiating spectrum is desirable for short pulse applications. The reflector IRA employs a paraboloidal reflector fed by TEM lines [11, 12], and is an example of an aperture antenna. It is well known that the radiated field from an aperture antenna consists of a spatial integration of the aperture fields over the aperture, while the temporal behaviour of the aperture field is differentiated in the far field. In a practical situation, the illuminating field or the aperture field is a double exponential waveform and the radiated field then becomes impulse-like with a very large bandwidth ratio. The reflector IRA under consideration

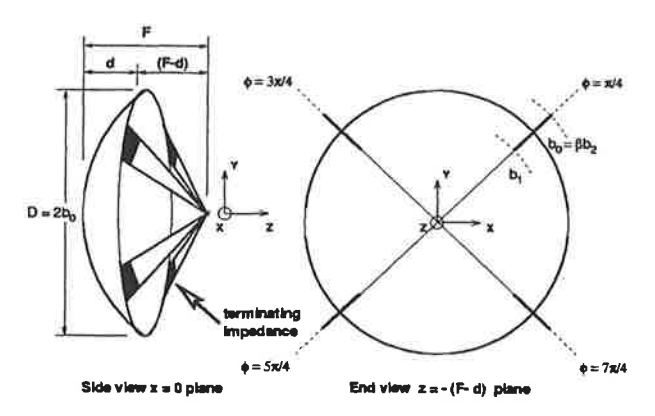


FIGURE 2 - An illustration of a reflector fed by a pair of coplanar conical TEM lines.

consists of a paraboloidal reflector fed by two pairs of coplanar feed plates as illustrated in figure 2. Coplanar feed plates are chosen over the more conventional facingplate geometry to minimize the aperture blockage effects. To reduce the aperture blockage, the feed plates are required to be narrow, resulting in feed impedances of several hundreds of Ohms. The 400Ω lines are connected in parallel resulting in a net feed impedance of 200 Ω . The aperture area should be as large as practically possible, since the far field E^f is proportional to the square root of this area for a constant voltage at the feed. The magnitude of the far field is proportional to the aperture area for a constant aperture field. The pulse generator has to be of the differential type to avoid common mode currents on the feed plates, which could distort the desired features in the far field. The driving voltage is $V(t) = (V_0/2)u(t)$, where V_0 is already defined in eqn. 2. Since $E^f \propto$ $\partial V/\partial t$, it is desirable to maximize this rate of rise of the incident field or the voltage pulse.

Two identical reflectors were manufactured with the following characteristics.

- one piece, spun aluminum, paraboloidal surface
- diameter $D = 900 \,\mathrm{mm}$
- focal length $F = 337.5 \,\mathrm{mm}$
- profile accuracy ≤ 1.5 mm
- $f_d = F/D = 0.375$

The desired rise time of 100 ps implies an upper 3 dB frequency of 3.5 GHz which gives rise to wavelengths in air of 85.7 mm. The surface tolerance of the reflector is small compared to the shortest wavelength and hence it is acceptable.

Next, we look at an estimation of boresight waveforms. For analysis purposes, one could consider a single (two conductor) coplanar feed, although in practice we used two such feed lines connected in parallel for a more uniform illumination of the reflector (see fig. 2). When the reflector IRA was originally proposed [5], the boresight radiation was predicted to consist of a feed step followed by an impulse-like behaviour. It was also shown that the total area under these two parts of the radiated waveform (i.e. prepulse plus impulse) is zero. This means, that there is no DC component in the radiated waveform consisting of the prepulse and the impulse. This further implies that the portion of the radiated waveform after the impulse must have a net zero area in itself. The post impulse portion consists of diffracted signals from the feed plate and the circular rim of the paraboloidal reflector. A more recent analysis [6] has extended this result by chronologically considering the various temporal elements of the boresight radiation, which is illustrated in figure 3. Let us assume that the voltage pulse generator is switched on at t = 0, and the observer is at a distance r(=z) to the right of the focal point of the paraboloid. These temporal elements are:

- Prepulse: feedstep $E_{y1}(r,t)$
- Main pulse: impulse $E_{y2}(r,t)$
- Postpulse:
 - feedplate diffraction: $E_{v3}(r,t)$ (actually this consists of two parts originating form the plate edge (3a) and the plate itself (3b))
 - edge diffraction from circular rim of the reflector, $E_{y4}(r,t)$
- Entire pulse constraints: low-frequency dipole moment radiation and no radiation at zero frequency (DC).

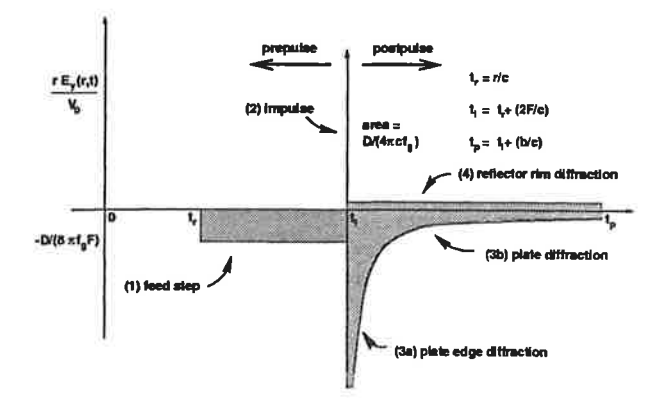


FIGURE 3 - On-axis radiation from a canonical reflector IRA.

The far field $\overrightarrow{E}^f(\overrightarrow{r},t)$ is given by,

$$\overrightarrow{E}^{f}(\overrightarrow{r},t) = \overrightarrow{l_{y}}E_{y}(r,t)$$
, where (6)

$$E_{y}(r,t) = \sum_{i=1}^{4} E_{yi}(r,t)$$
 (7)

+ low-frequency radiation from dipole moments resulting in time-integral constrains on entire pulse.

Detailed, closed-form expressions for the components $E_{yi}(r,t)$ in the above expression, are available in [7]. The results of eqn. 6 is illustrated in fig. 3. The time-integral constraints imposed by the low-frequency radiation are,

- the complete first-time integral of the radiated waveform must be zero, and
- ii) the second-time integral must be proportional to the late-time dipole moments.

Feed plates, terminating and matching

The feedplates form a parallel combination of $2 \times 400 \Omega$ conical TEM lines, giving the IRA an input impedance of 200 Ω . Matching to the 50 Ω pulse source is done by means of a balun. Suitable high-frequency, high-voltage, and high-impedance cables are difficult to find. Finally a 100Ω flexible cable with a PTFE dielectric was chosen. The latter is bound to introduce some dispersion, however the cable can be replaced by a better one in the future. Terminiation of each feed plate at the dish edge consists of a net DC impedance of 200Ω . The insulating spacer is a high density polyethylene slab the dimensions of which are optimised experimentally. Capacitance of the slab is trimmed by drilling holes (tuned with help of TDR measurements at the antenna terminal). The Terminating resistor network, consist of a series-parallel network (5 by 5) of 1 W, 200Ω carbon composite resistors of 10% tolerance. Thus total heat dissipation is not a problem. Since the length of the resistor chain is ≥ 10 cm, the voltage stand-off (in the order of 10 kV/cm) is not seen to be a problem either.

Far field of the IRA

If an aperture antenna of diameter D is illuminated by a CW field of frequency f, then the far field is determined by the distance r such that,

$$r \ge \frac{2D^2}{\lambda},\tag{8}$$

which is obtained by requiring that $\Delta_r \leq (\lambda/16)$ where Δ_r is the path difference of the edge ray and the central ray from aperture to observer. For pulsed antennas we define a clear time $t_c = \Delta_r/c$ and we associate far field conditions at a distance where $t_c < t_{\rm rise}$, in which $t_{\rm rise}$ denotes the rise time of the incident pulse at the aperture. It is verified that

$$t_c = \frac{1}{c} \left[\sqrt{\frac{D^2}{4} + r^2} - r \right]. \tag{9}$$

TABLE 1 - Clear time t_c for a reflector diameter $D=0.9\,\mathrm{m}$ with respect to distance

	r	Δ_r	$t_c = \Delta_r/c$
	(in m)	(in mm)	(in ps)
- 0	1.0	96	320.0
	2.0	50	166.6
	2.5	40	133.3
	3.0	33	110.0
	3.5	29	96.6
	4.0	25	83.3
	5.0	20	66.6
	8.0	12	40.0
	10.0	10	33.3

Requiring that $t_c < t_{rise}$, it is observed from table 1 that the observation point has to be greater than 8 m, to be in the far field, by a comparison of the clear time with the rise time of 100 ps. The radiated fields on the bore-sight are known in closed form in the far field [5, 6, 7, 8, 9]. More recently, Russian researchers [14] have worked out near and far field expressions of the E-field on the boresight of an IRA. Using these expressions, we have estimated the on-axis E-field at various distances in the near and far field of the antenna. This is the subject of the next subsection. Although 8 m is the minimum distance to be in the far field, the actual experiments of illuminating targets can be performed at shorter distances in the near field. The pulse is broader and has more low-frequency components in the near field. In fact, very near the antenna, for example at the feed point, the electric field is similar to the voltage pulse which is a double exponential waveform. The differentiation occurs in the far field and the transformation from near to far field is gradual and not abrupt. This transformation can be experimentally observed by measuring the electromagnetic field on-axis, as one moves away from the focal region. These values have been experimentally veri-

TABLE 2 - Near field and far field characteristics of the IRA (bore-sight)

IKA (boic-sig	111)	
quantity	near field	far field
distance R	5 m	10 m
clear time	66 ps	33.3 ps
prepulse	-255 V/m	-127 V/m
prepulse duration	$2.25\mathrm{ns}$	2.25 ns
impulse peak	5.9 kV/m	$3.8\mathrm{kV/m}$
impulse duration	85 ps	60 ps

fied during initial measurements and compare favourably with the above table. Expressions for the radiated spectrum are available in literature as mentioned earlier. Calculations for our IRA results in the values tabulated in table 3. Measurements indicate that due to practical restrictions the actual performance is not quite as good as theoretically expected.

TABLE 3 - Calculated bore-sight values for a distance

	O 111
E	$=2.85 \cdot 10^{-7} \text{ V/m (+/- 12\%)}$
f_l (3dB)	$= 80 \mathrm{MHz}$
f_u	$= 10 \mathrm{GHz}$
BW-ratio	= 125
decades	= 2.097

UWB GPR EXPERIMENTAL FACILITY

To perform experiments in a controlled environment, a full scale experimental/test facility was erected on the premises of TNO-FEL. This facility has been developed in cooperation with the Delft University of Technology and will be used to illuminate objects buried in a realistic sand medium with an ultra-wideband electromagnetic field. The electromagnetic field scattered by the buried object has to be recorded and diagnosed for the benefit of developing a computer database containing the responses of a large number of potential targets (i.e. land-mines etc.).

The experimental facility consists of a buried wooden box. The dimensions of this box are $10 \,\mathrm{m} \times 10 \,\mathrm{m}$ wide and 3 m deep. Special care has been taken not to use any metal parts in the construction of the box or in the vicinity thereof. The sand-box is filled with clean homogeneous river sand. In order to keep the condition of the sand in the box optimal and to prevent pollution from the outside (for example ground water) entering the box, a drainage system was installed and the inside of the box was covered with a watertight plastic lining. To prevent the weather from influencing the test conditions and to protect the measuring equipment, a large tent covers the entire site. While filling the box with sand, special care was taken to get a homogeneous profile. Current tests indicate that this was not entirely successful but should be good enough to work with. Later on we might choose to empty the box and refill it with a ground (soil) of a different composition. To facilitate the measurement of EM transmissions into the ground a square PVC tube running from the surface of one side to the bottom of the other side has been installed about one meter from the edge of the sand-box.

EXPERIMENTAL RESULTS

In this section we present results obtained from an AT-mine located on the surface (sand) at the experimental facility previously described. We have stacked the data to reduce the influence of noise. For each A-scan we have used 8 pulses. An example of such an A-scan is shown in figure 5. The B-scan is presented in figure 6, in which one can easily see the presence of the AT-mine. The B-scan starts 2 m before and stops 2 m after the mine. It is noted that for the sake of symplicity we have moved the mine instead of the antennas. In this experiment, we have used a horizontal increments of 2 cm.

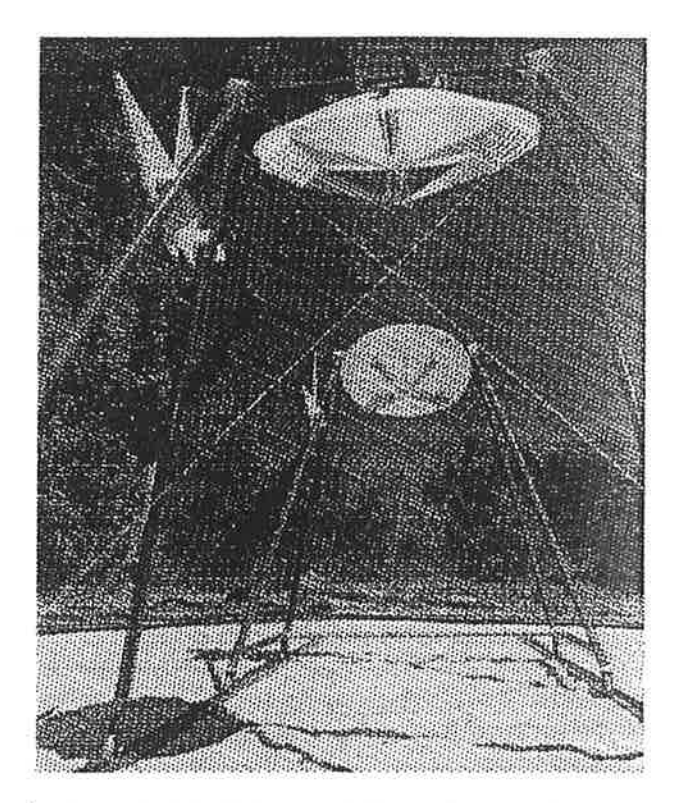


FIGURE 4 - The IRAs mounted on A-frames at the UWB GPR experimental facility.

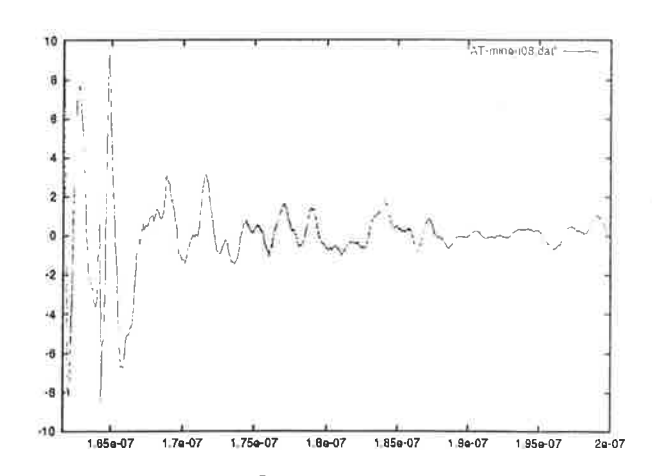


FIGURE 5 - A-scan of an AT-mine recorded by the UWB GPR system described

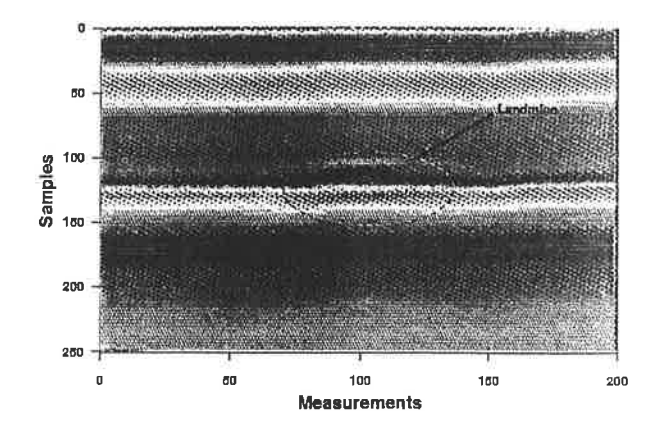


FIGURE 6 - B-scan of an AT-mine recorded by the UWB GPR system descibed

The UWB GPR system developed at TNO-FEL offers a versatile and open experimental platform for implementing signal processing algorithms for mine detection and identification. The sand-box test facility plays a crucial part in the evaluation of the system. The experimental results recently obtained shows that the design specification and theoretical projections are sufficiently satisfied. The mechanical structure of the IRA is somewhat delicate, especially in the feeding point. Nevertheless, we feel that the main advantages of the IRA are the ultra wide bandwidth, fast rise time and high energy bandwidth that are favourable for detection and classification of buried objects. The singularity expansion method (SEM) was tried on synthetic data and promisses to be a powerful tool in the identification of landmine signatures. SEM along with other algorithms will be implemented and evaluated on the TNO-FEL UWB GPR system in the near future.

REFERENCES

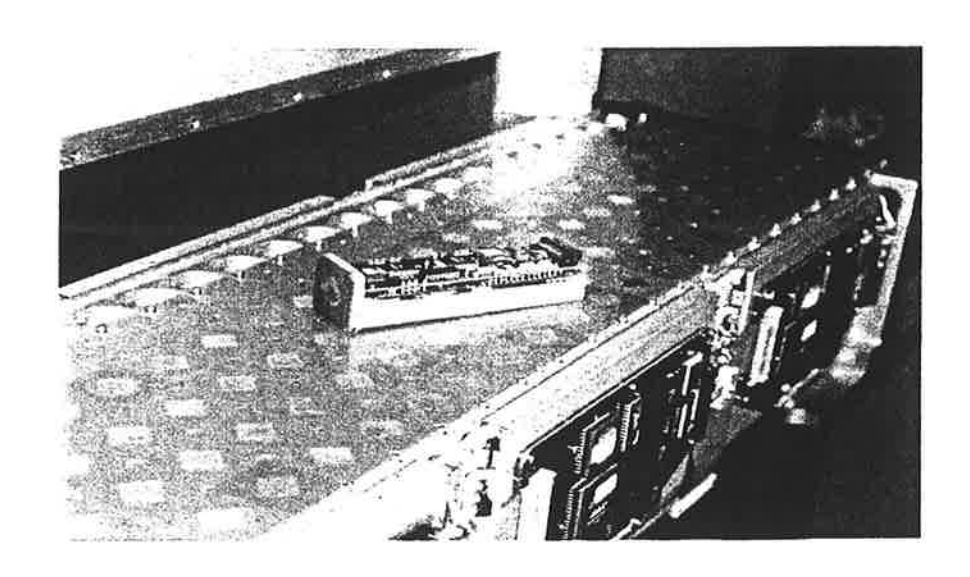
- [1] J. LoVetri, S. Primak, B.J.A.M. van Leersum and A.P.M. Zwamborn, June 1998, "Feasibility study into the identification of land-mines using UWB radar and analysis using synthesized data", presented at <u>EUROEM'98</u>, Tel Aviv, to be published in "Ultra-Wideband Short-Pulse Electromagnetics 4"
- [2] C.E. Baum, E.J. Rothwell, K.M. Chen and D.P. Nyquist, 1991, "The Singularity Expansion Method and its application to target identification", <u>Proc. of the IEEE, vol. 79, no. 10, pp. 1481–1492</u>
- [3] C.E. Baum,1994, "Signature-based target identification and pattern recognition", <u>IEEE Antennas and Propagation Magazine</u>, vol. 36, no. 3, pp. 44–51
- [4] C.E. Baum, L. Carin and A.P. Stone, 1996, "Ultrawideband short-pulse electro-magnetics 2", <u>Plenum</u> Press, New York, ISBN 0-306-45502-X.
- [5] D.V. Giri and C.E. Baum, "Temporal and spectral radiation on bore-sight if a reflector type of impulse radiating antenna (IRA)", published in [4].
- [6] D.V. Giri and C.E. Baum, November 1989, "Radiation of impulse-like transient fields", Sensor and Simulation Notes, no.321.
- [7] D.V. Giri and C.E. Baum, February 1994. "Reflector IRA design and bore-sight temporal waveforms", Sensor and Simulation Notes, no. 365 1
- [8] D.V. Giri, H. Lackner, I.D. Smith, D.W. Morton, C.E. Baum, J.R. Marek, D. Scholfield and W.D. Prather, July 1995, "A reflector antenna for radiating impulse-like waveforms", Sensor and Simulation Notes, no. 382
- [9] D.V. Giri, November 1995, "Radiated spectra of impulse radiating antennas (IRAs)", <u>Sensor and</u> Simulation Notes, no. 386

- 37
- [11] C.E. Baum, D.V. Giri and R.D. Gonzalez, April 1976, "Electromagnetic field distribution of the TEM mode in a symmetrical two-parallel plate transmission line", <u>Sensor and Simulation Notes</u>, no. 219
- [12] F.C. Yang and L. Marin, September 1977, "Field distribution on a two-conical plate and a curved cylindrical plate line", <u>Sensor and Simulation</u> Notes, no. 229
- [13] J.J.A. Klaasen, August 1992, "An efficient method for the performance analysis of bounded-wave nuclear EMP simulators", <u>Sensor and Simulation</u> Notes, no. 345
- [14] O.V. Mikheev, S.A. Podosenov, K. Yu. Sakharov, A.A. Sokolov, Ya.G. Svekis and V.A. Turkin, "New method for calculating pulse radiation from an antenna with a reflector", submitted to IEEE Transactions on Electromagnetic Compatibility

^{1.} The "Sensor and Simulation Notes" can be obtained from the Phillips Laboratory, Kirtland AFB, NM 87117, USA

FLM Od Bogaaut

International Symposium on ANTENNAS FOR RADAR EARTH OBSERVATION



Symposium Proceedings

Held on the occasion of the inauguration of Prof. P. Hoogeboom, at Delft University of Technology, the Netherlands, 8–9th June 2000.



8-9th June 2000 Delft University of Technology



International Research Centre for Telecommunications-Transmission and Radar